

Comparative study of fiber optic liquid level sensors based on long-period fiber gratings with different doping concentrations

Barerem-Melgueba Mao^{1*}, Yizhen Wei (魏一振)¹, and Bin Zhou (周斌)^{1,2}

¹Centre for Optical and Electromagnetic Research, Zhejiang University, Hangzhou 310058, China

²Institute of Optics, Zhejiang University, Hangzhou 310027, China

*Corresponding author: francoismao@gmail.com

Received October 20, 2011; accepted December 12, 2011; posted online March 6, 2012

The performances of two liquid level sensors based on long-period fiber gratings are studied. The long-period gratings (LPGs) have similar characteristics (length and period), but are fabricated with two photosensitive B-Ge co-doped fibers with different dopant concentrations. We investigate the temperature sensitivities of LPGs and exploit their refractive index sensitivity to implement liquid level measurement. By controlling fiber parameters, such as the dopant concentrations, the measurement sensitivity of a LPG-based fiber optic liquid level sensor can be improved.

OCIS codes: 050.2770, 060.2370, 230.1150.

doi: 10.3788/COL201210.050501.

Liquid level sensing (i.e., the measurement of liquid volume) has been intensely studied as a gauging technique because of its essential applications in modern industry. For example, in a refinery or chemical plant, large numbers of liquid level sensors (LLSs) are usually employed to monitor liquid storage tanks. A mass of systems, like aircraft fuel gauging and ink jet printing, also rely on liquid level measurement to enable proper functioning. The properties of a liquid, such as being flammable or inert, must be carefully considered in designing LLSs because they can result in diverse types of sensors for different applications. LLSs can be generally classified by their mechanisms: mechanical^[1], electrical^[2], and optical^[3–5]. Among these techniques, optical fiber-based LLSs present some remarkable advantages, such as their immunity to electromagnetic interference, high sensitivity, and resistance to rugged environments. Optical fiber-based sensors are lightweight and small in size. They are especially attractive for applications in explosive environments and flammable atmospheres because light is confined inside the fiber, a dielectric material, and does not interact with the surrounding material. Recently, LLS based on long-period grating (LPG) has attracted considerable attention due to its simplicity and reliability. LPG is a type of fiber device that couples light between the fundamental core mode and forward-propagating cladding modes. This coupling results in a transmission spectrum consisting of a series of attenuation bands at distinct wavelengths^[6]. These attenuation bands are sensitive to temperature, strain^[6], bending curvature^[7], and the refractive index (RI) of the surrounding material^[8]. The purpose of LPG-based sensors is to measure the wavelength shift of a specific attenuation band while one of the external physical parameters (i.e., temperature, strain, bend, and RI) is changing.

In this letter, we compare the performances of fiber optic LLSs based on long-period fiber gratings. Two LPG-based LLSs were fabricated using two B-Ge co-doped fibers with different doping concentrations. These LLSs were carefully studied in the application of liquid level

sensing with different solutions. The temperature sensitivities of the LPGs were also measured. The experimental results show that the fiber dopant concentrations have significant effects on the shift of the resonance wavelengths of the LPG. Our work provides valuable insight into the mechanism of LPG-based LLS, as well as an approach to improve measurement sensitivity.

LPGs are obtained by introducing a periodic modulation of the RI in the core of photosensitive fibers, with a spatial period ranging from 100 μm to 1 mm. The light coupling between core mode and the co-propagating cladding modes occurs at distinct wavelengths given under the phase matching condition as^[9]

$$\lambda_l = [n_{\text{core}}^{\text{eff}}(\lambda_l) - n_{\text{clad},l}^{\text{eff}}(\lambda_l)]A, \quad (1)$$

where λ_l is the coupling wavelength, A is the period of the LPG, $n_{\text{core}}^{\text{eff}}$ is the effective index of the propagating core mode, and $n_{\text{clad},l}^{\text{eff}}$ is the effective index of the l th cladding mode susceptible to the RI of surrounding medium. When variations of external physical parameters, such as RI, alter the LPG's period and/or the core-cladding index difference, the phase-matching condition is changed, resulting in a wavelength shift of the transmission dips. Using LPG-based LLS, one can measure the liquid level by detecting the wavelength shift, which depends on surrounding medium's RI. Changes in resonant wavelength according to the surrounding medium's RI (n_{ext}) can be expressed as^[10]

$$\frac{d\lambda_l}{dn_{\text{ext}}} = \lambda_l \gamma \Gamma_{\text{ext}}, \quad (2)$$

where γ is the general sensitivity factor and is given by

$$\gamma = \frac{(d\lambda_l/dA)}{n_{\text{core}}^{\text{eff}} - n_{\text{clad},l}^{\text{eff}}}, \quad (3)$$

where γ is positive for low-order cladding modes, whereas it is negative for high-order cladding modes. The symbol

Γ_{ext} represents the RI sensitivity factor and is defined as

$$\Gamma_{\text{ext}} = -\frac{u_l^2 \lambda_l^3 n_{\text{ext}}}{8\pi r_{\text{clad}}^3 n_{\text{clad}} (n_{\text{core}}^{\text{eff}} - n_{\text{clad},l}^{\text{eff}}) (n_{\text{clad}}^2 - n_{\text{ext}}^2)^{3/2}}, \quad (4)$$

where u_l is the l th root of the zero-order Bessel function of the first kind; r_{clad} and n_{clad} are the radius and the RI of the fiber cladding, respectively; Γ_{ext} is always negative for $n_{\text{ext}} < n_{\text{clad}}$.

Temperature is an important factor that is always involved in sensing. The wavelength dependence on temperature can be derived as^[6]

$$\frac{d\lambda_l}{dT} = \frac{d\lambda_l}{d(\delta n_{\text{eff}})} \left[\frac{dn_{\text{core}}^{\text{eff}}}{dT} - \frac{dn_{\text{clad},l}^{\text{eff}}}{dT} \right] + \lambda_l \frac{d\lambda_l}{d\lambda} \frac{1}{L} \frac{dL}{dT}, \quad (5)$$

where λ_l is the central wavelength of the attenuation band, T is the temperature, L is the length of LPG, and $\delta n_{\text{eff}} = (n_{\text{core}}^{\text{eff}} - n_{\text{clad},l}^{\text{eff}})$ denotes the core-cladding index difference.

In our experiments, we fabricated two LPGs (LPG1 and LPG2) with the same length ($L = 50$ mm) and period ($\Lambda = 460$ μm), but using different fibers. LPG1 was fabricated in a photosensitive B-Ge co-doped fiber (fibercore PS 1250/1500) consisting of 10% of GeO_2 and 20% of B_2O_3 , whereas the fiber used to fabricate LPG2 had a different doping concentration of GeO_2 (28.277%) and B_2O_3 (2.375%). Both fibers were not hydrogen-loaded. The gratings were obtained by exposing each fiber to ultraviolet (UV) irradiation using a point-by-point technique. A KrF excimer laser with 248-nm wavelength was employed as the UV source. An optical spectrum analyzer (ANDO AQ6317) and a broadband light source (KFA1a-S04) were used for measuring the transmission spectra of the LPGs. The insets of Fig. 1 show the transmission spectra of our LPGs placed in air at room temperature (25 °C). The main transmission dips (i.e., the transmission dips that exhibit the highest attenuation) of LPG1 and LPG2 are at 1532 and 1579 nm, respectively. By calculation, the two transmission

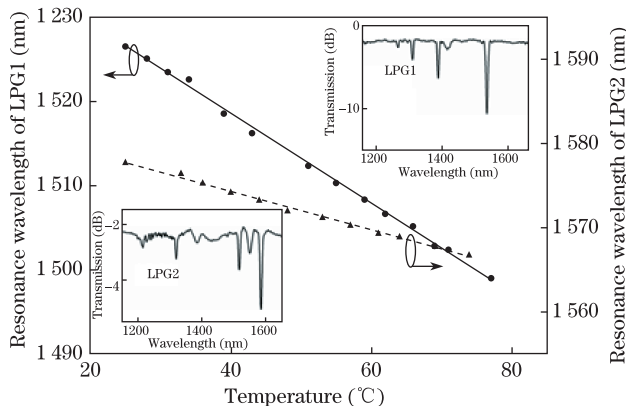


Fig. 1. Measured temperature dependence of resonance wavelength of LPGs. The solid line represents the temperature dependence of the resonance wavelength (at $\lambda=1532$ nm) for LPG1; the dashed line represents the temperature dependence of the resonance wavelength (at $\lambda=1579$ nm) for LPG2. The insets show the transmission spectra in air at room temperature of LPG1 and LPG2.

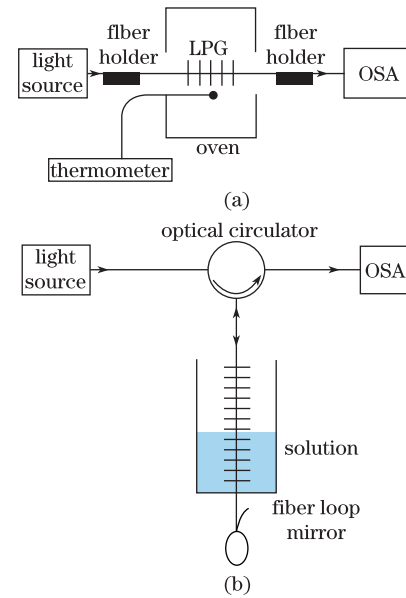


Fig. 2. Experimental setups for the measurement of (a) temperature-induced wavelength shifts and (b) the liquid level.

dips correspond to the same order cladding mode^[11,12]. Furthermore, we measure the temperature sensitivities (in air) of these cladding modes, and our results are in agreement with those obtained in Refs.[11–13]. These two dips were considered in our experiments.

We have investigated the thermal response (in air) of each LPG, using the setup shown in Fig. 2(a). A broadband light source was connected to one end of the LPG, and an optical spectrum analyzer was employed to measure the transmission spectrum from the other end. The LPG was properly fixed in an oven that achieved temperature controlling together with a thermometer. As shown in Fig. 1, the temperature was varied from 25 to 75 °C, and the central wavelength of the attenuation band was shifted continuously from 1526.48 to 1499.73 nm for LPG1 and from 1577.66 to 1566.48 nm for LPG2, respectively.

We obtained the temperature sensitivities after linear fitting. For LPG1, the temperature sensitivity of the dip at 1532 nm was -0.531 nm/°C, whereas for LPG2 we recorded a sensitivity of -0.228 nm/°C for the dip at 1579 nm. The measured temperature sensitivities are in good agreement with results of other papers^[11,13]. Because LPG1 and LPG2 have the same length and period and the two transmission dips correspond to the same cladding mode, the difference of fiber dopant concentrations should be the origin of the difference in the temperature sensitivities obtained.

The sensitivity of LPG to RI was used to detect the level of liquid, in which the grating is partially or completely immersed. For this purpose, two solutions were used: pure water with a RI of 1.3329 and a solution of glycerol with a RI of 1.4069. Figure 2(b) shows the experiment setup, which is under constant temperature during the whole test. In contrast to most of other LPG-based LLSs, we studied the shift of the central wavelength of the attenuation bands in order to eliminate the power instability issues (induced, for example, by the power fluctuation of light source) when the trans-

mission spectrum was recorded. This method creates a stable and high-resolution fiber optic sensor. During the level detection tests, the wavelength shift was observed continuously using an optical spectrum analyzer with a resolution of 0.05 nm.

Figure 3 shows the resonance wavelength shift of the LPGs as a function of the percentage of the LPGs' length immersed in the solutions. Figure 4 shows the transmission spectra of LPG1 and LPG2 with different solutions as the surrounding medium. For both LPGs, the wavelengths of resonant bands present a blue shift with increasing liquid level, which can be explained by Eqs. (2)–(4). For the low-order cladding modes, the term $\frac{d\lambda_l}{dn_{\text{ext}}}$ is negative, resulting in a blue wavelength shift with the increase of the external RI, as we observed in the experiment. The change of surrounding medium's RI modifies the effective RI of LPG's cladding modes, which is very sensitive to external variations. The resonance wavelength will then experience a shift in order to satisfy the phase-matching condition. When the level of water covering the gratings gradually rose from 0% (LPG

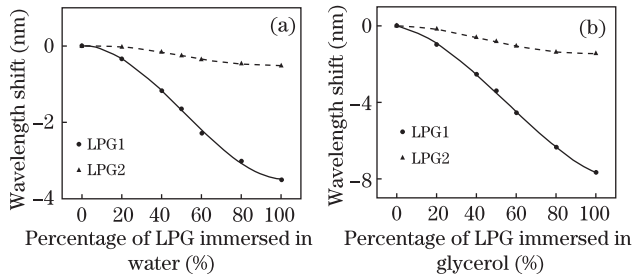


Fig. 3. Measured LPGs' resonance wavelength shift with different liquid levels in (a) water (RI=1.3329) and (b) glycerol (RI=1.4069). The solid line represents the liquid level dependence of the resonance wavelength (at $\lambda=1532$ nm) shift for LPG1; the dashed line represents the liquid level dependence of the resonance wavelength (at $\lambda=1579$ nm) shift for LPG2.

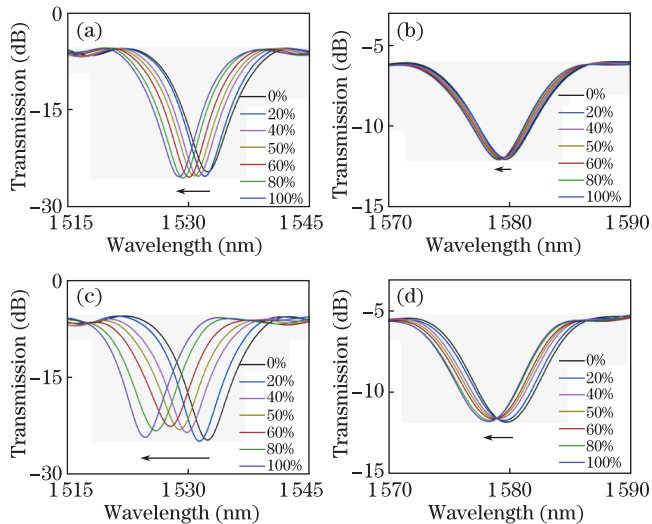


Fig. 4. (Color online) Transmission spectra of LPG1 (at 1532-nm resonance) and LPG2 (at 1579-nm resonance) for different levels of immersion in solutions. (a) LPG1 and (b) LPG2 in water (RI=1.3329); (c) LPG1 and (d) LPG2 in glycerol (RI = 1.4069).

in air) to 100% (LPG fully immersed in solution), the resonant band of LPG1 at 1532 nm experienced a total shift of 3.5 nm, whereas a much smaller wavelength shift of 0.52 nm was observed by using LPG2 (resonant band at 1579 nm). In glycerol solution, we observed a total shift of 7.69 nm for LPG1, whereas it was 1.47 nm for LPG2. For the same level with different liquid surrounding the LPGs, the larger wavelength shift was observed in glycerol solution, which had a larger RI. As a result, greater wavelength shift can be obtained with larger RI of the liquid under detection. Considering the attenuation bands studied in the experiment, LPG1 was observed to be more sensitive to external RI change and to the liquid level. The RI sensitivity of the grating (for $n_{\text{ext}} < n_{\text{clad}}$) increases as the RI of its surrounding medium increases, as demonstrated in Ref.[14]. Equations (2)–(4) show that, after derivation, when the surrounding medium's RI (n_{ext}) increases, sensitivity also increases. This trend was also observed experimentally. The experimental results are in good agreement with the theoretical predictions. By changing the doping concentrations in the photosensitive fiber, one can change the differential effective index ($n_{\text{core}}^{\text{eff}} - n_{\text{clad},l}^{\text{eff}}$). The surrounding material's effects on the cladding modes' effective RI are then changed. The attenuation band's resonant wavelength shift would then also change. Because the differential effective index is always positive, Eq. (4) shows that the sensitivity to the external RI increases as the differential effective index decreases.

In conclusion, we demonstrate two different LLSs using long-period fiber gratings with the same characteristics but fabricated using different B-Ge co-doped photosensitive fibers of different dopant concentrations. The performances of the two LLSs are compared. The experimental results show that fiber parameters, such as the doping concentrations, have significant effects on the wavelength shift of the attenuation bands of LPG and can enhance the sensitivity of the LLSs. By controlling fiber parameters, such as the doping concentrations, one can improve the sensitivity of fiber optic LLSs based on LPGs.

The authors acknowledge Prof. Aping Zhang from Zhejiang University for his help and advice. This work was supported by the National Natural Science Foundation of China under Grant No. 60907020.

References

1. B. W. Northway, N. H. Hancock, and T. Tran-Cong, *Meas. Sci. Technol.* **6**, 85 (1995).
2. F. N. Toch, G. C. M. Meijer, and M. van der Lee, in *Proceedings of the Conference on Precision Electromagnetic Measurements Digest* 356 (1996)
3. J. A. Morris and C. R. Pollock, *J. Lightwave Technol.* **5**, 920 (1987).
4. K. Iwamoto and I. Kamata, *Appl. Opt.* **31**, 51 (1992).
5. S. Khaliq, S. W. James, and R. P. Tatam, *Opt. Lett.* **26**, 1224 (2001).
6. V. Bhatia, D. K. Campbell, D. Sherr, T. G. D'Albarto, N. A. Zabaronick, G. A. Ten Eyck, K. A. Murphy, and R. O. Claus, *Opt. Eng.* **36**, 1872 (1997).
7. C. C. Ye, S. W. James, and R. P. Tatam, *Opt. Lett.* **25**, 1007 (2000).

8. H. J. Patrick, A. D. Kersey, and F. Bucholtz, *J. Lightwave Technol.* **16**, 1606 (1998).
9. A. M. Vengsarkar, P. J. Lemaire, J. B. Judkins, V. Bhatia, T. Erdogan, and J. E. Sipe, *J. Lightwave Technol.* **14**, 58 (1996).
10. X. Shu, L. Zhang, and I. Bennion, *J. Lightwave Technol.* **20**, 255 (2002).
11. X. Shu, T. Allsop, B. Gwandu, L. Zhang, and I. Bennion, *IEEE Photon. Technol. Lett.* **13**, 818 (2001).
12. M. Smietana, W. J. Bock, and P. Mikulic, *Meas. Sci. Technol.* **21**, 025309 (2010).
13. A. I. Kalachev, D. N. Nikogosyan, and G. Brambilla, *J. Lightwave Technol.* **23**, 2568 (2005).
14. J. H. Chong, P. Shum, H. Haryono, A. Yohana, M. K. Rao, C. Lu, and Y. Zhu, *Opt. Commun.* **229**, 65 (2004).